2D RF Ion Thruster Modeling with Fluid Plasma and Analytical Sheath Formulation

Emre Turkoz*, Murat Celik†
Bogazici University, Istanbul, 34342, Turkey
emre.turkoz@boun.edu.tr

SP2014_2980764

Abstract

This paper discusses the modeling of the inductively coupled plasma (ICP) in RF ion thruster discharge chamber. The model handles the three species, which are electrons, ions and neutrals, as ideal gas and formulates fluid equations to solve for the flow field parameters. Continuity and momentum equations are solved for all species whereas an energy equation is solved only for electrons. Ions and neutrals are assumed as cold, constant temperature gas species. Electric and magnetic fields inside the discharge chamber are evaluated by solving a magnetic vector potential equation. The model is implemented for a 2D axisymmetric geometry and equations are discretized with finite volume method in cylindrical coordinates. To deal with the real-world experiment conditions, a matching circuit model is added, where the coupling between the plasma and the external circuits are handled through approximating the plasma as the secondary of an air-core transformer. The model equations extend up to the presheath region where the plasma is quasi-neutral. For the sheath region an analytical formulation is presented to evaluate the potential drop. The validation of the model is performed using the commercial software, COMSOL. It is demonstrated that the model can be used to evaluate the performance of various thruster designs accurately.

I. Introduction

Radio-frequency (RF) ion thrusters are plasma-based impulse generators for in-space applications. RF ion thrusters consist of a discharge chamber, which contains the plasma, and the electric circuitry implemented around this discharge chamber to handle the power deposition and RF heating. Example geometries of a conical and a cylindrical shaped discharge chamber can be seen in Fig.1. The necessary energy deposited into the partially ionized gas comes from the RF coils, which generates the inductively coupled plasma. Screen and accelerator grids can be seen on the right end of the discharge chamber, which accelerate ions out of the discharge chamber. Manufacturing of these grids is also subject to a great effort, since a great precision is required in the machining process. The grids can be made of several materials, such as molybdenum and carbon, whereas the discharge chamber is generally made of dielectric materials, such as quartz. Neutral xenon gas is fed from the left end. Neutral xenon atoms get ionized with the energy provided by the RF coils. The output from the discharge chamber is neutralized with a cathode, which can be seen aiming towards the plume of the thruster.

The RF ion thrusters are first invented in the 1960s in Germany [1]. Giessen University was the host of this invention. After that, Astrium GmbH, a private German company, has adopted this development and managed to build thrusters which can be used in space missions. The most advanced product of these early efforts was RIT-10, which has a 10 cm discharge chamber diameter. RIT-10 is space tested in 1992. This spacetest was performed on the EURECA carrier. RIT-10 was incorporated into the European ARTEMIS satellite, which was sent to the space for geo-stationary communication purposes. RIT-10 is lifetime tested for 15,000 hours in 2000. The com-

*Graduate Student, Department of Mechanical Engineering, Bogazici University
†Assistant Professor, Department of Mechanical Engineering, Bogazici University.

mercially available RIT-10 package is also called as *RITA* [2].

After the development of the RIT-10 ion thruster, German Space Agency (DARA) has started a project in 1995 for RIT-15, which has a 15 cm chamber diameter and is planned to deliver specific impulse more than 4000 seconds at 50 mN of thrust [1]. This amount of specific impulse enables the application area of large geostationary satellites and platforms for RF ion thrusters.

Miniaturization of RF ion thrusters are performed in the late 2000s. Astrium GmbH and their partners in the academy developed RIT-μX, which is built for micropropulsion applications in 2007 [3]. In 2011, researchers from Giessen University and Moscow Aviation Institute designed a very large ion thruster, RIT-45, which has a discharge chamber diameter of 46.5 cm [4]. RIT-45 works with 35 kW power and delivers a specific impulse of 7000 s.

Plasma physics simulations are relatively new in the modeling world, since most of the underlying physics is subject to further investigation. Numerical treatment of inductively coupled plasma is performed numerous times in the literature. Electromagnetic heating is the core of the process, which is again elaborated in many examples. Two application areas, plasma processing and plasma torch modeling, come forward for the fields that have similar physics as RF ion thrusters. Examples in the literature about these fields are very helpful in building a numerical model for RF plasma.

There are few numerical models for ion thrusters in general, and there are models for inductively coupled plasma, but the number of models for RF ion thruster is very limited. A leading example [5] is based on evaluating the discharge loss per ion with an analytical model. The 0D model described in that work is simple but successful at predicting the performance of ion thrusters in real applications. It lays out the effect of the induced magnetic field due to the RF coils on the ion confinement and discusses factors that result in a decrease in the discharge loss per ion. Another recent 0D model [6] indicates a trade-off between mass utilization efficiency and power transfer efficiency with increasing gas flow rate.

Additional to the analytical models, there are also one or multi-dimensional RF ion thruster discharge chamber modeling studies. A simple transformer model [7] is first laid out for 1D modeling, assuming that the thruster is large enough to assume 1D approach could be valid. Then this model is extended to a 2D model [8] which evaluates the plasma parameters of RF ion thrusters with the help of additional experimental data specific for the thruster to be modeled. In that study, the plasma is treated as a continuum as it is treated in the same way as in this work.

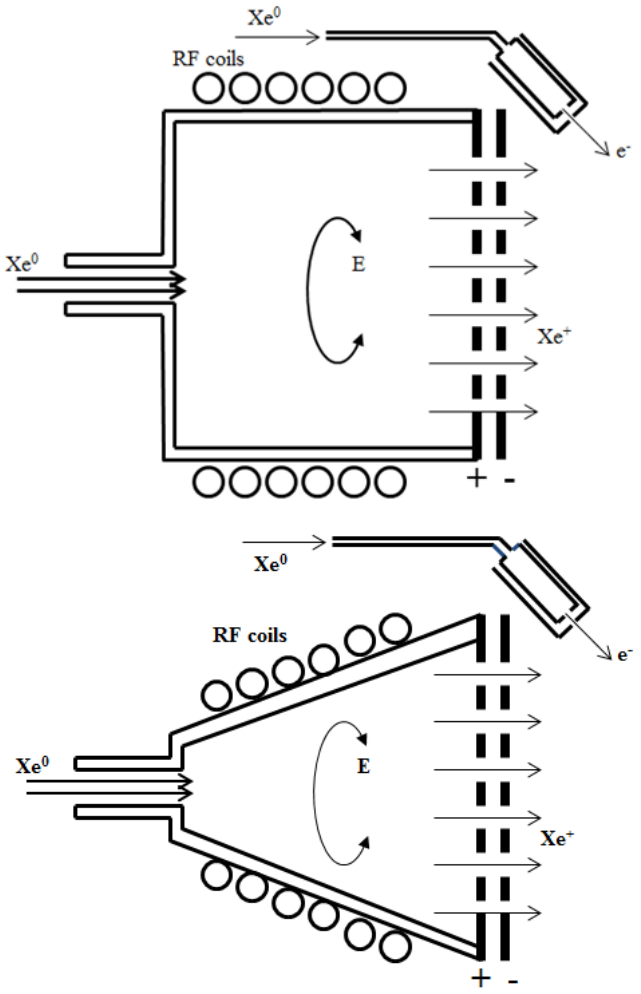

Figure 1: Representation of the cylindrical and conical discharge chambers

There are also studies with the kinetic approach, using a PIC (Particle-In-Cell) code to solve for the spatial distribution of the plasma parameters. An example model [9] is developed to evaluate the performance of the micro RF ion thrusters. A 3D fully kinetic model [10], that requires strong computation power, is laid out recently for RF ion thrusters.

Using a PIC code is always possible but the usage of the fluid approach decreases the computational cost drastically. Plasma must obey the continuum approach for the fluid modeling to be possible. The investigation of the question whether the inductively coupled plasma inside the RF ion thruster discharge chamber obeys the continuum approach is already performed [8]. Therefore a fluid model is developed in this work. The model presented in this work consists of three main components: Electromagnetic model, fluid model and the transformer model. The electromagnetic model handles the solution of the

Maxwell equations, the fluid model evaluates the flow of the plasma and the transformer model evaluates the matching circuit parameters and most importantly the alternating current magnitude to be supplied to the RF coils.

In this study a new numerical model that relies on the fluid assumption for plasma is presented and verified with a commercial software. The governing equations are solved on a 2D cylindrical and axially symmetric domain. The details of this model is given in Section II. The numerical method utilized to solve the model equations is explained in Section III. Section IV is dedicated for the results and concluding remarks are given in Section V.

II. Theory Model

A model, which consists of electromagnetic, fluid, and transmformer submodels, is previously described in [11]. The equations utilized in this model are listed here again.

Continuity equations for ion and neutral number densities (n_i and n_n):

$$\frac{\partial n_i}{\partial t} + \nabla\cdot(n_i\mathbf{v_i}) = \dot{R} \tag{1}$$

$$\frac{\partial n_n}{\partial t} + \nabla\cdot(n_n\mathbf{v_n}) = -\dot{R} \tag{2}$$

Momentum equations for ion and neutral velocities ($\mathbf{v}_i$ and $\mathbf{v}_n$):

$$m_i n_i\left(\frac{\partial \mathbf{v_i}}{\partial t} + \mathbf{v_i}\cdot\nabla\mathbf{v_i}\right) + k\nabla(n_iT_i) = en_i\mathbf{E} + en_i\mathbf{v_i}\times\mathbf{B} - m_in_i\nu_{in}(\mathbf{v_i}-\mathbf{v_n}) - m_in_i\nu_{ei}(\mathbf{v_i}-\mathbf{v_e}) \tag{3}$$

$$m_n n_n\left(\frac{\partial \mathbf{v_n}}{\partial t} + \mathbf{v_n}\cdot\nabla\mathbf{v_n}\right) + k\nabla(n_nT_n) = - m_nn_n\nu_{in}(\mathbf{v_n}-\mathbf{v_i}) - m_nn_n\nu_{en}(\mathbf{v_n}-\mathbf{v_e}) \tag{4}$$

Electron flux ($\mathbf{\Gamma}_e$) using drift-diffusion:

$$\mathbf{\Gamma}_e = -\frac{k\nabla(n_eT_e)}{m_e\nu_{eff}} + \frac{en_e}{m_e\nu_{eff}}(\nabla\phi - v_{e,\theta}\times\mathbf{B}) \tag{5}$$

The electron temperature (T_e) is evaluated by solving the power balance for electrons:

$$\frac{3}{2}\frac{\partial}{\partial t}(n_eeT_e) + \nabla\cdot\mathbf{Q_e} = -e\mathbf{E_a}\cdot\mathbf{\Gamma_e} + P_{dep} - P_{coll} \tag{6}$$

The electromagnetic fields are evaluated by solving the magnetic vector potential ($\mathbf{A}$) equation:

$$\nabla^2\mathbf{A} = \mu_0\sigma\frac{\partial\mathbf{A}}{\partial t} \tag{7}$$

where $\dot{R}$ denotes the ion generation through first ionization collision and is formulated as $\dot{R} = n_nn_e\langle\mathbf{v_e}Q_{ion}\rangle$. The term in angled brackets is the ionization reaction rate obtained from [12] for Xenon. In momentum equations ν_{ei}, ν_{en} and ν_{in} denote the electron-ion, electron-neutral and ion-neutral collision frequencies, respectively. The magnetic vector potential is defined so that it satisfies $\nabla\times\mathbf{A} = \mathbf{B}$ and $\nabla\cdot\mathbf{A} = 0$. The energy balance equation (6) contains the heat flux due to conduction, which is formulated as given in [13]:

$$\mathbf{Q}_e = \frac{5}{2}\mathbf{\Gamma}_eeT_e - \frac{5}{2}\frac{n_ee^2T_e}{m_ev_{eff}}\nabla T_e \tag{8}$$

Power deposition is formulated as:

$$P_{dep} = \sigma|\mathbf{E}|^2 \tag{9}$$

The power loss term due to elastic and inelastic collisions is formulated as:

$$P_{coll} = n_en_ne\langle\mathbf{v}_eQ_{ion}\rangle U_{ion} + n_en_ne\langle\mathbf{v}_eQ_{exc}\rangle U_{exc} + \sum_h^{heavy}\frac{2m_e}{m_h}\frac{3}{2}k(T_e-T_h)\nu_{eh}n_e \tag{10}$$

where, U_{ion} is the first ionization energy, U_{exc} is the average excitation energy, and the terms in angled brackets represent the reaction rates. The electric potential, ϕ, is evaluated by inserting the drift-diffusion approximation that contains this term into the current continuity equation, which is $\nabla\cdot\mathbf{j} = \nabla\cdot(e\mathbf{\Gamma}_i - e\mathbf{\Gamma}_e) = 0$.

Additional to these equations, a transformer model to represent the matching circuit is added into the simulation. This transformer model is implemented as described in [8] and [14].

The sheath potential drop incident on the floating walls can be calculated using the zero-current condition on the walls. According to this condition, the ion and electron fluxes incident on the wall should be equal:

$$n_su_B = n_s\frac{\bar{c}_e}{4}\exp\left(\frac{e\Delta\phi}{kT_e}\right) \tag{11}$$

where n_s denotes the plasma density at the sheath edge, $\Delta\phi$ is the sheath potential drop between the wall and the sheath edge, and $u_B = \sqrt{kT_e/m_i}$ is the Bohm velocity for ions at the sheath edge.

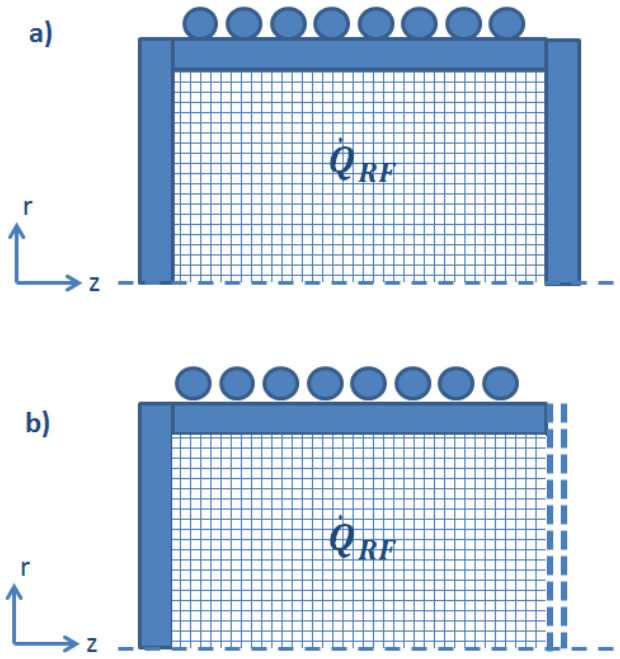

Figure 2: Representation of the domains solved in this study. a) ICP discharge confined withing dielectric walls for verification. b) ICP discharge in an ion thruster, where an electrostatic grid is placed to the right end of the domain

According to this formulation, the sheath potential drop is:

$$\Delta\phi = -\frac{kT_e}{e}\ln\left(\sqrt{\frac{m_i}{2\pi m_e}}\right) \tag{12}$$

The floating sheaths for the configurations investigated in this study are collisionless and low-pressure sheaths. Using the Child-Langmuir Law presented in [15], the sheath thickness can be expressed as:

$$s = \frac{2}{3}(\Delta\phi)^{3/4}\left(\frac{J_i}{\epsilon_0}\right)^{-1/2}\left(\frac{2e}{m_i}\right)^{1/4} \tag{13}$$

where $J_i = en_iu_B$ denotes the ion current density entering the sheath. The sheath potential drop and the sheath thickness allow for the calculation of the electric potential distribution inside the sheath by solving the following nonlinear differential equation:

$$\frac{d^2\phi}{dx^2} = -\frac{J_i}{\epsilon_0}\left(-\frac{2e\phi(x)}{m_i}\right)^{-1/2} \tag{14}$$

where the boundary condition at the plasma boundary ($x = s$) is taken to be zero, and the boundary condition on the wall ($x = 0$) is taken to be the sheath potential drop, $\Delta\phi$. The above equation is a form of the Poisson's equation, where the right hand side is replaced with the net space charge expression assuming that $n_e = 0$ in regards to the Child-Langmuir law. The ion density can be calculated as:

$$n_i(x) = n_s\left[1 - \left(\frac{2e\phi(x)}{m_iu_B^2}\right)\right]^{-1/2} \tag{15}$$

The Child-Langmuir approach assumes that the electron number density is negligible compared to the ion number density. But an approximation for the electron density can be evaluated using the Boltzmann's relation:

$$n_e(x) = n_s\exp\left(\frac{e\phi(x)}{kT_e}\right) \tag{16}$$

where n_s is the plasma density at the sheath edge.

In this study two different configurations are handled as depicted in Fig. 2. The first configuration represents the verification case, where the ICP is confined within dielectric walls. This pseudo-chamber with no inlets is considered to have RF power deposited into the plasma with ions undergo a recombination and become neutrals at the discharge boundaries. The nonequilibrium ICP discharge is solved with COMSOL Plasma Module and AETHER software that is developed in the scope of this study, and the results from both platforms are used for verification.

The second configuration is the representation of an RF ion thruster, where the right dielectric wall is replaced with grids for acceleration. This configuration is investigated to understand the discharge characteristics of an ion thruster.

III. Numerical Method

The equations presented in Section II. are discretized on a structured rectangular grid in 2D cylindrical coordinates for an axially symmetric domain. Continuity and momentum equations are solved using the finite volume method. The species are assumed to behave as ideal gas, and the finite volume method is applied as presented in [16] and adapted for compressible gases as presented in [17]. The remaining equations are discretized according to the second order finite differencing scheme and the resulting linear systems are solved self-consistently.

The second-order finite differencing and finite volume discretizations on structured rectangular grids in 2D yield coefficient matrices that have a penta-diagonal sparsity pattern. The coefficient matrices are stored using the compressed diagonal storage (CDS) method [18]. The resulting linear systems are solved using ILU-GMRES method [19].

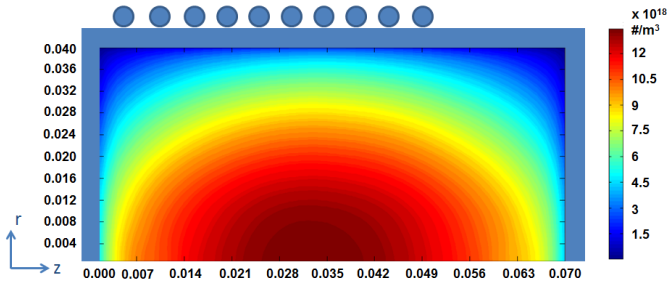

Figure 3: Plasma density at the end of 10 miliseconds. Due to the losses to the walls, plasma is confined in the center region of the domain

The nonlinear equation (14) to evaluate the electric potential inside the sheath is solved with Newton's method. The Jacobian matrix is evaluated explicitly by first evaluating the derivative of the discretization of this equation, which is performed using second order finite differencing.

IV. Results

The model explained in previous sections of this work is used to solve a benchmark ICP configuration to verify the results with the Plasma Module of the commercial software COMSOL. For the verification, the preferred discharge chamber is a cylinder made of a dielectric, which is 7 cm long and has a diameter of 8 cm. RF power is deposited into the plasma through the 10 coil windings around the chamber, which extends 5 cm in axial direction. Driving frequency is 13.56 MHz. Argon is the type of the gas. Initial pressure is 20 mTorr, which corresponds to 3.0E+20 m^{-3} neutral density. There is no neutral gas inlet to the system. All the ions that reach the wall go through a recombination process and directed back into the system as neutrals. The same configuration is solved also with COMSOL and the results are compared. For comparison, two different power deposition values, that result in steady-state solutions, are chosen. These values are 3500 W and 6000 W.

The plasma density distribution obtained from AETHER at 10 miliseconds is shown in Fig. 3. It is seen that the plasma is confined at the center of the discharge chamber because of the losses to the walls. It is also seen that the plasma density is slightly higher in the regions that are located below the coils (from origin to 0.050 m in axial direction) compared to regions that do not lay under RF coils (from 0.050 m to 0.070 m in axial direction).

The verification is performed by taking the data on two lines and comparing the electron number density values along these lines for different power deposition values.

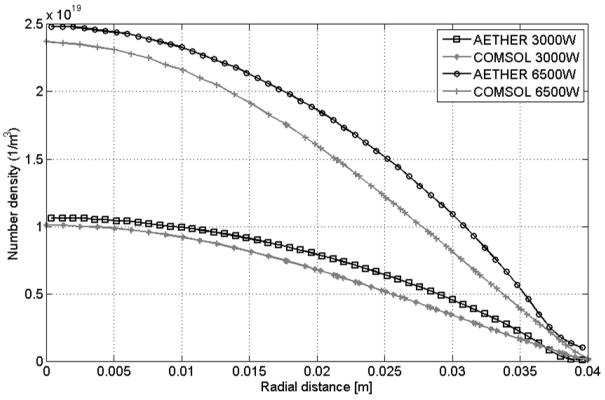

Figure 4: *Comparison of number density results from AETHER and COMSOL along the line L1 for 3000 W and 6500 W.*

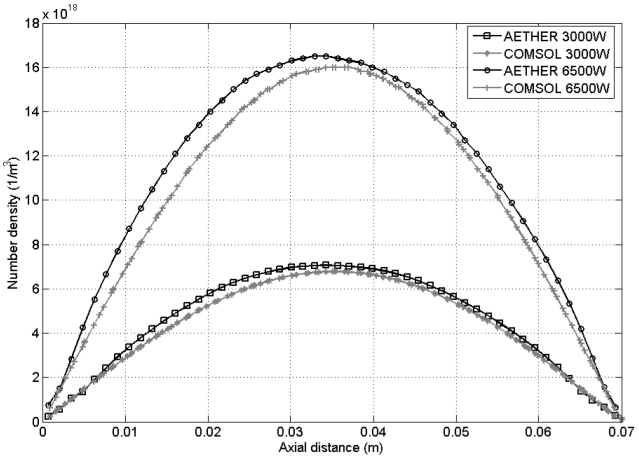

Figure 5: *Comparison of number density results from AETHER and COMSOL along the line L2 for 3000 W and 6500 W.*

The first line, $L_1 = |P_1P_2|$, is the center line in radial direction, which starts at $P_1 = (0.035, 0.000)$ and extends up to $P_2 = (0.035, 0.040)$. The number density values along the line L_2 are presented in Fig. 4. The second line, $L_2 = |P_3P_4|$, is the center line in axial direction, which starts at $P_3 = (0.000, 0.020)$ and extends up to $P_4 = (0.070, 0.020)$. The number density values along the line L_2 are presented in Fig. 5.

The RF ion thruster simulations are performed for a very similar configuration in terms of geometry. An example thruster configuration, which is very similar to RIT-15LP [20], is modeled. This thruster has 15 cm diameter and 7 cm axial length. The coil wrapped around the cylindrical discharge chamber is represented on the axisymmetric domain with 13 equidistant coils. The RF frequency is 2 MHz, which means that one RF cycle is $5.0e-07$ sec. Two different pressure levels are tested by applying 4 sccm and 13 sccm neutral flow rates for inlet gas.

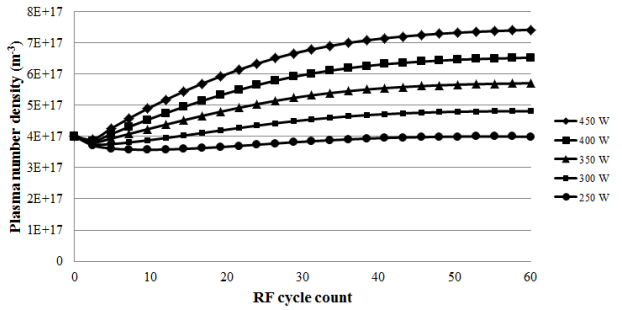

Figure 6: *Plasma density vs. time for 4 sccm neutral flow rate at different power levels*

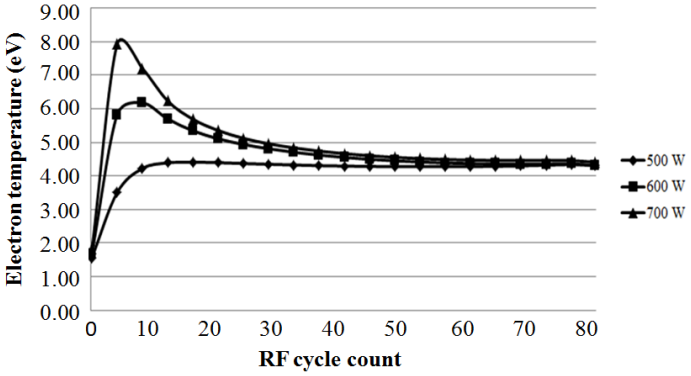

Figure 7: *Mean temperature change vs. time for 13 sccm neutral flow rate at different power levels*

Five different power deposition cases are tested with 250-, 300-, 350-, 400- and 450-W power deposition values for 4 sccm neutral Xenon gas inflow. The plasma densities for these power deposition values are depicted in Fig. 6. The mean electron temperature for these power depositions does not vary significantly and can be taken as 3.08 eV.

When the Xenon gas mass flow rate and the background neutral pressure are increased, a higher power deposition is required to sustain the plasma as expected. With the same discharge chamber geometry, the steady-state temperature is this time much higher along with the power deposition. To observe the effect of high pressure, the neutral flux is increased from 4 sccm to 13 sccm. The tested power deposition values that yield steady-state solutions are 500-, 600- and 700-W. As it is observed with the previous configuration, the electron temperature yields average values which are very close for each case. The average temperature change for each case versus time is presented in Fig. 7. For the 600 W case, the mean electron temperature is 4.31 eV.

The sheath region is not resolved with the 2D axisymmetric numerical model as stated in previous sections. The analytical method outlined in Section II. is applied for the 4.31 eV bulk plasma electron temperature and $1e+17\ m^{-3}$ presheath plasma density. The sheath width is calculated as $8.4538e-05$ meters, and the total sheath potential drop is 13.07 V. The electron and ion number density distributions in the sheath region are given in Fig. 8. The electric potential distribution in the sheath is presented in Fig. 9.

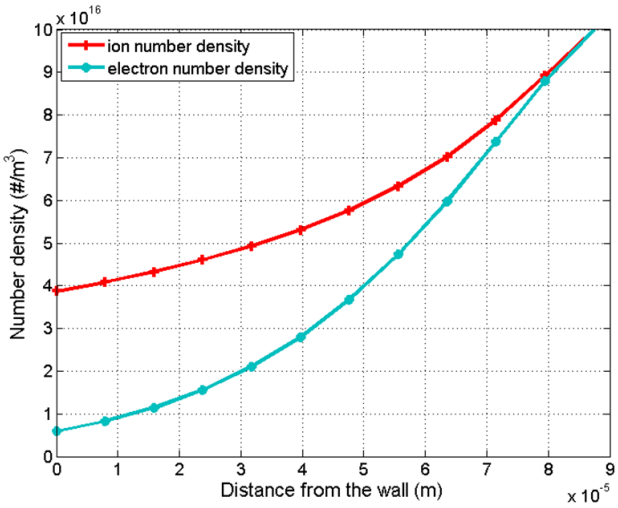

Figure 8: *Number densities in the sheath region*

V. Conclusions

A fluid model of the plasma inside the dishcarge chamber of an RF ion thruster is built that does not require any empirical input.

The results lay out that the electron temperature inside an RF ion thruster discharge chamber is almost constant for various power levels at the same pressure. The beam current increases with the increasing power, and this increase can be attributed to the increase of the plasma density and the ionization fraction.

There is a nonlinear relation between electron temperature, chamber dimensions, plasma density and the beam current. Thruster efficiency should also be taken into account and an optimization study should be carried out to evaluate the best configuration for RF ion thrusters.

The analytical sheath model presented in this study serves currently only for post-processing purposes. It is used to monitor the change in species number densities and electric potential inside the sheath region. A possible coupling of this analytical formulation with the heat loss boundary condition of the fluid model should be investigated in the future.

An extension of the code can be possible if the capability to capture the electrostatic fields in plasma

is implemented. This can also lead to the simulation of various types of plasma sources where the nonambipolar flow is dominant. The simulation of these type of flows could be possible if electrons are solved separately from the ions and the electric potential can be evaluated by solving the Gauss' Law. An attempt to these simulations is to be found in [21]. The interested reader should also consider reading the different sheath phenomena observed in these types of plasma [22].

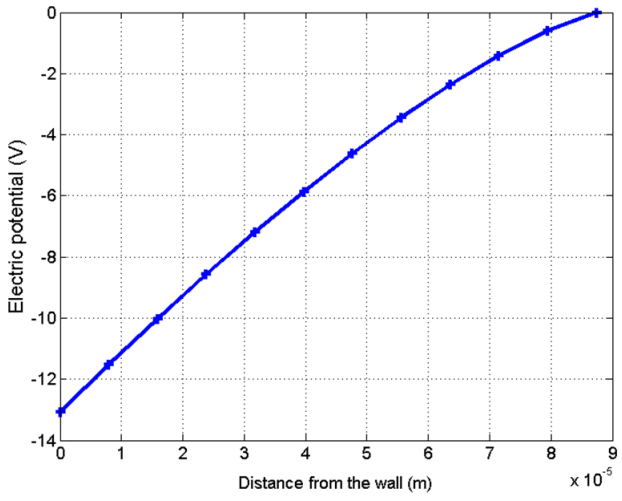

Figure 9: *Electric potential in the sheath region*

Acknowledgement

This research is supported by Turkish Scientific and Technological Reseach Council (TUBITAK) under projects 112M862 and 113M244 and partially by Bogazici University Scientific Projects Office under project number BAP-6184. The authors would like to thank Prof. Huseyin Kurt of Istanbul Medeniyet University for allowing the usage of the computational facilities at Istanbul Medeniyet University and the COMSOL Multiphysics software for this study.

References

[1] Groh, K. H., Leiter, H. J., and Loeb, H. W., "RIT15-A medium Thrust Range Radio-Frequency Ion Thruster," 2^{nd} *European Space Propulsion Conference*, ESTEC, Noordwijk, Netherlands, 1997, pp. 252–257.

[2] Killinger, R., Mller, J., Kukies, R., and Bassner, H., "RITA Ion Propulsion for ARTEMIS–Lifetime Test Results," *Spacecraft Propulsion*, Vol. 465, 2000, pp. 433.

[3] Leiter, H., Killinger, R., Boss, M., Braeg, M., Gollor, M., Weis, S., Feili, D., Tartz, M., Neumann, H., and Cara, D. M. D., "RIT–μT – High Precision Micro Ion Propulsion System Based on RF-Technology," 43^{rd} *Joint Propulsion Conference and Exhibit*, Cincinnati, OH, July 2007, AIAA–2007–5250.

[4] Loeb, H. W., Feili, D., Popov, G. A., Obukhov, V. A., Balashov, V. V., A. I. Mogulkin, V. M. Murashko, A. N. N., and Khartov, S., "Design of High–Power High–Specific Impulse RF–Ion Thruster." 32^{nd} *International Electric Propulsion Conference*, 2011, also IEPC–2011–290.

[5] Goebel, D., "Analytical Discharge Model for RF Ion Thrusters," *IEEE Transactions on Plasma Science*, Vol. 36, No. 5, October 2008, pp. 2111 –2121.

[6] Chabert, P., Monreal, J. A., Bredin, J., Popelier, L., and Aanesland, A., "Global Model of a Gridded-Ion Thruster Powered by a Radiofrequency Inductive Coil," *Physics of Plasmas*, Vol. 19, No. 4, 2012, pp. 1–8, 073512.

[7] Tsay, M. and Martinez-Sanchez, M. M., "Simple Performance Modeling of a Radio-Frequency Ion Thruster," 30^{th} *International Electric Propulsion Conference*, Florence, Italy, September 2007, IEPC–2007–072.

[8] Tsay, M., "Two-Dimensional Numerical Modeling of Radio-Frequency Ion Engine Discharge," Ph.D. Thesis, Massachusetts Institute of Technology, Cambridge, MA, USA, 2011.

[9] Takao, Y., Eriguchi, K., and Ono, K., "Two-Dimensional Particle-in-Cell Simulation of a Micro RF Ion Thruster," 32^{nd} *International Electric Propulsion Conference*, Wiesbaden, Germany, September 2011, IEPC-2011-076.

[10] Henrich, R. and Heiliger, C., "Three Dimensional Simulation of Micro Newton RITs," 33^{rd} *International Electric Propulsion Conference*, Washington, DC, October 2013, IEPC–2013–301.

[11] Turkoz, E. and Celik, M., "2D Electromagnetic and Fluid Models for Inductively Coupled Plasma for RF Ion Thruster Performance Evaluation," *IEEE Transactions on Plasma Science*, Vol. 42, No. 1, Jan 2014, pp. 235–240.

[12] Goebel, D. M. and Katz, I., *Fundamentals of Electric Propulsion - Ion and Hall Thrusters*, JPL Space Science and Technology Series, 2008.

[13] Kawamura, E., Graves, D. B., and Lieberman, M. A., "Fast 2D hybrid fluid-analytical simulation of inductive/capacitive discharges," *Plasma*

Sources Science and Technology, Vol. 20, No. 3, 2011, pp. 035009.

[14] Piejak, R., Godyak, V., and Alexandrovich, B., "A simple analysis of an inductive RF discharge," *Plasma Sources Science and Technology*, Vol. 1, No. 3, 1992, pp. 179.

[15] Chabert, P. and Braithwaite, N., *Physics of Radio-Frequency Plasmas*, University Press, Cambridge, 2011.

[16] Versteeg, H. and Malalasekera, W., *An Introduction to Computational Fluid Dynamics - The Finite Volume Method*, Prenctice Hall, Essex, England, 1995.

[17] Ferziger, J. H. and Peric, M., *Computational Methods for Fluid Dynamics, 3rd Edition*, Springer-Verlag, Berlin, 2002.

[18] Barrett, R., Berry, M. W., Chan, T. F., Demmel, J., Donato, J., Dongarra, J., Eijkhout, V., Pozo, R., Romine, C., and Van der Vorst, H., *Templates for the solution of linear systems: building blocks for iterative methods*, SIAM, 1994.

[19] Meijerink, J. and van der Vorst, H. A., "An iterative solution method for linear systems of which the coefficient matrix is a symmetric M-matrix," *Mathematics of computation*, Vol. 31, No. 137, 1977, pp. 148–162.

[20] Leiter, H., Loeb, H., and K.H.-Schartner, "RIT15LS and RIT15LP – The Development of High Performance Mission Optimized Ion Thrusters," 35^{th} *Joint Propulsion Conference and Exhibit*, Los Angeles, CA, June 1999, AIAA–99–2444.

[21] Zhu, Y., "Modeling of a microwave plasma electron source for neutralization of ion thrusters," Ph.D. Thesis, Paul Sabatier University of Toulouse, France, 2013.

[22] Baalrud, S. D., Hershkowitz, N., and Longmier, B., "Global Nonambipolar Flow: Plasma Confinement where All Electrons are Lost to One Boundary and All Positive Ions to Another Boundary," *Physics of Plasmas*, Vol. 14, No. 042109, 2007, pp. 1–6.